Supporting Information

Homogeneously Dispersed Co_9S_8 Anchored on Nitrogen and Sulfur Co-Doped Carbon Derived from Soybean as Bifunctional Oxygen Electrocatalysts and Supercapacitor

*Zhen Xiao[1†], Guozheng Xiao[1], Minhao Shi[1], Ying Zhu[1,2]**

[1]Key Laboratory of Bio-Inspired Smart Interfacial Science and Technology of Ministry of Education, School of Chemistry, Beihang University, Beijing, 100191, P.R. China

[2]Beijing Advanced Innovation Center for Biomedical Engineering, Beihang University, Beijing, 100191, P.R. China.

Email: zhuying@buaa.eud.cn

Experimental

Characterizations. The morphologies of the cobalt-containing freeze-dried soybeans and CoS@NSC-X catalysts were observed by Field Emission Scanning Electron Microscopy (FESEM, JEOL7500) and Transmission Electron Microscopy (TEM, JEOL JEM-2100F). Molecular structures of all samples were characterized by X-ray photoelectron spectroscopy (XPS), X-ray diffraction (XRD) and Raman spectroscopy. XPS spectra were collected on the Thermo Scientific ESCALab 250Xi using 200 W monochromated Al Kα radiation. TZY-XRD (D/MAX-TTR□, Cu Kα) was used to get the XRD pattern. Raman spectra were recorded on a JobinYvon (Laboratory RAM HR1800) confocal micro-Raman spectrometer backscattered geometry through a 10×(NA=0.25) microscope objective. An Ar^+ laser emitting at a wavelength of 514.5 nm was used as a source of excitation. Thermo-gravimetric analysis (TGA) analysis of dried rose petals was carried out on Thermo-LABSYS evo TGA sensor in nitrogen atmosphere. Nitrogen absorption/desorption isotherm was performed with ASAP 2020M (Micromeritics, USA) to obtain Bunauer-Emmett-Teller (BET) specific surface area. The pore size distribution was obtained from the adsorption branch of the isotherms derived from the Barrett-Joyner-Halenda (BJH) analysis.

Table S1. The XPS elemental analyses of the as-prepared samples

	C1s	O1s	N1s	S2p	Co2p
Soybean Precursor	60.76%	22.4%	6.92%	2.54%	/
NSC-700	78.73%	14.4%	4.91%	1.29%	/
NSC-800	83.11%	14.22%	1.83%	0.74%	/
NSC-800	85.45%	12.59%	0.96%	0.18%	/
CoS@NSC-700	78.13%	10.67%	9.2%	1.96%	1.05%
CoS@NSC-800	85.02%	8.14%	5.31%	1.82%	0.78%
CoS@NSC-900	89.19%	6.97%	2.2%	1.15%	0.55%

Table S2. Content of different types of nitrogen in CoS@NSC-700, CoS@NSC-800 and CoS@NSC-900 based on the high-resolution spectra of N1s.

	CoS@NSC-700	CoS@NSC-800	CoS@NSC-900
Pyridine N	21.4%	23.5%	26.8%
Pyrrolic N	45.5%	25.3%	50.6%
Graphitic N	24.3%	43.4%	17.5%
Oxidized N	8.8%	7.8%	5.1%

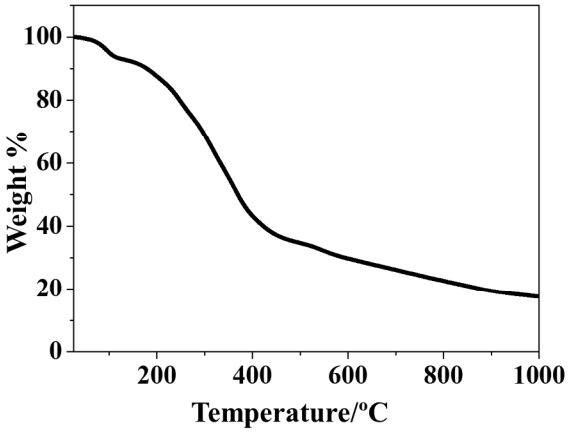

Figure S1. Thermogravimetric analysis curve of soybean precursor after KOH-$(NH_4)_2S_2O_8$ treatment.

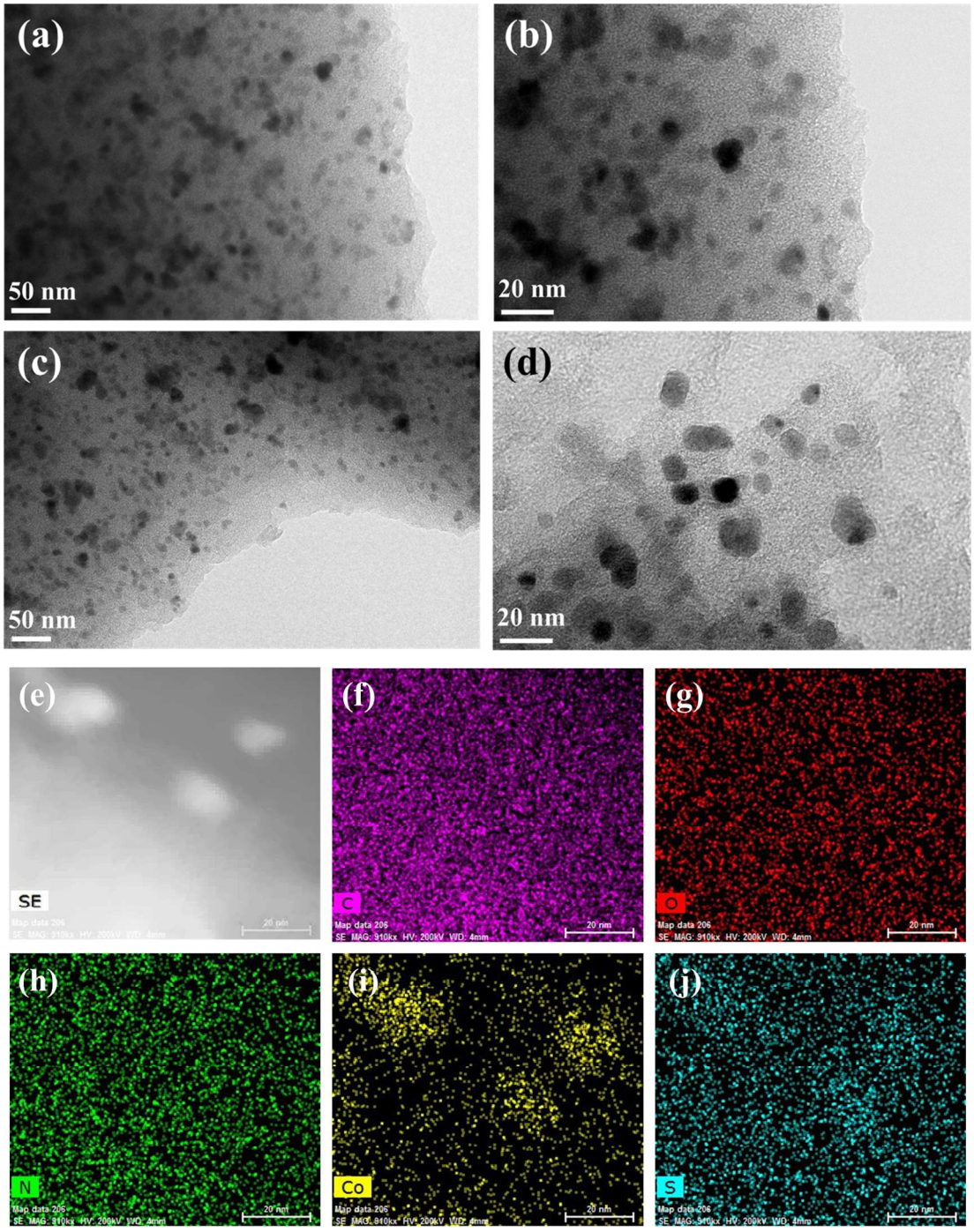

Figure S2. TEM images of the as-prepared CoS@NSC-700 (a, b) and CoS@NSC-900 (c, d); (e-k) the element mapping images for CoS@NSC-800.

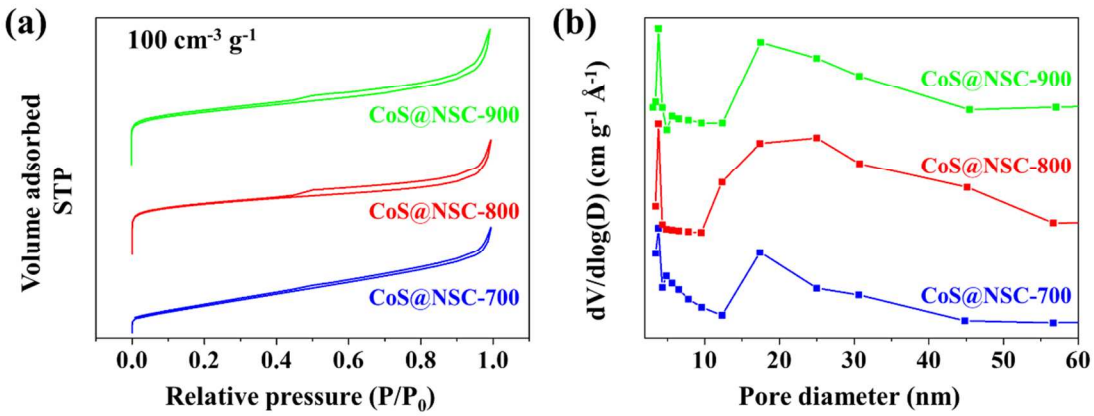

Figure S3. (a) The Nitrogen adsorption-desorption isotherms of CoS@NSC-700, CoS@NSC-800 and CoS@NSC-900. (b) The corresponding pore-size distribution by analysis of adsorption branch using Barrett-Joyner-Halenda (BJH) method.

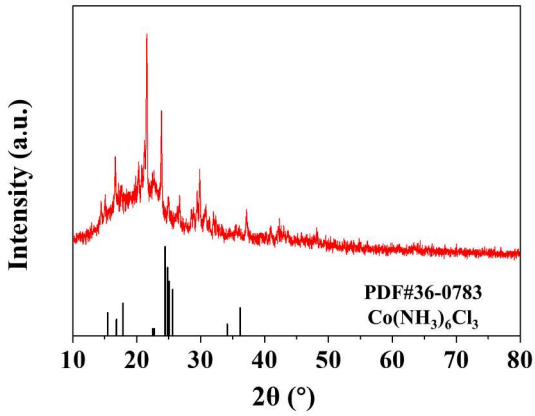

Figure S4. The XRD pattern of soybean precursor after KOH-$(NH_4)_2S_2O_8$ treatment.

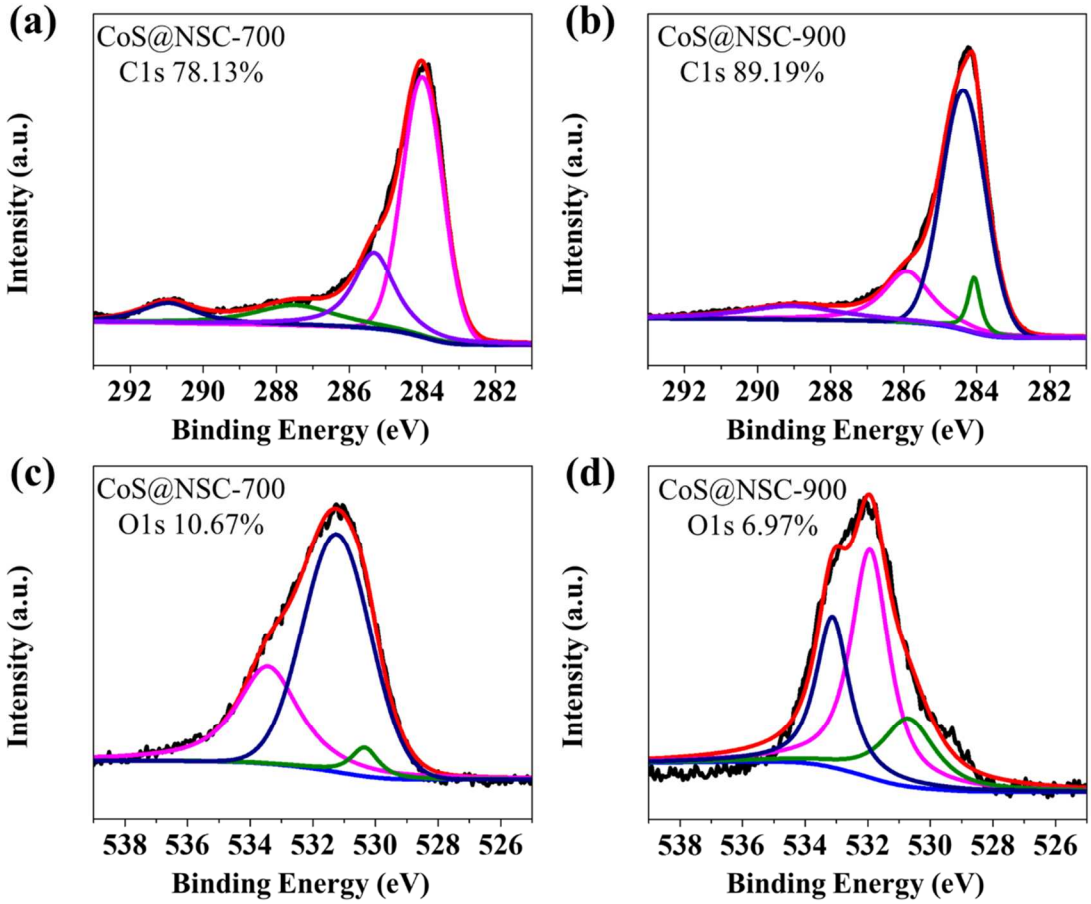
(a)
CoS@NSC-700
C1s 78.13%
Intensity (a.u.)
292 290 288 286 284 282
Binding Energy (eV)
(b)
CoS@NSC-900
C1s 89.19%
Intensity (a.u.)
292 290 288 286 284 282
Binding Energy (eV)
(c)
CoS@NSC-700
O1s 10.67%
Intensity (a.u.)
538 536 534 532 530 528 526
Binding Energy (eV)
(d)
CoS@NSC-900
O1s 6.97%
Intensity (a.u.)
538 536 534 532 530 528 526
Binding Energy (eV)

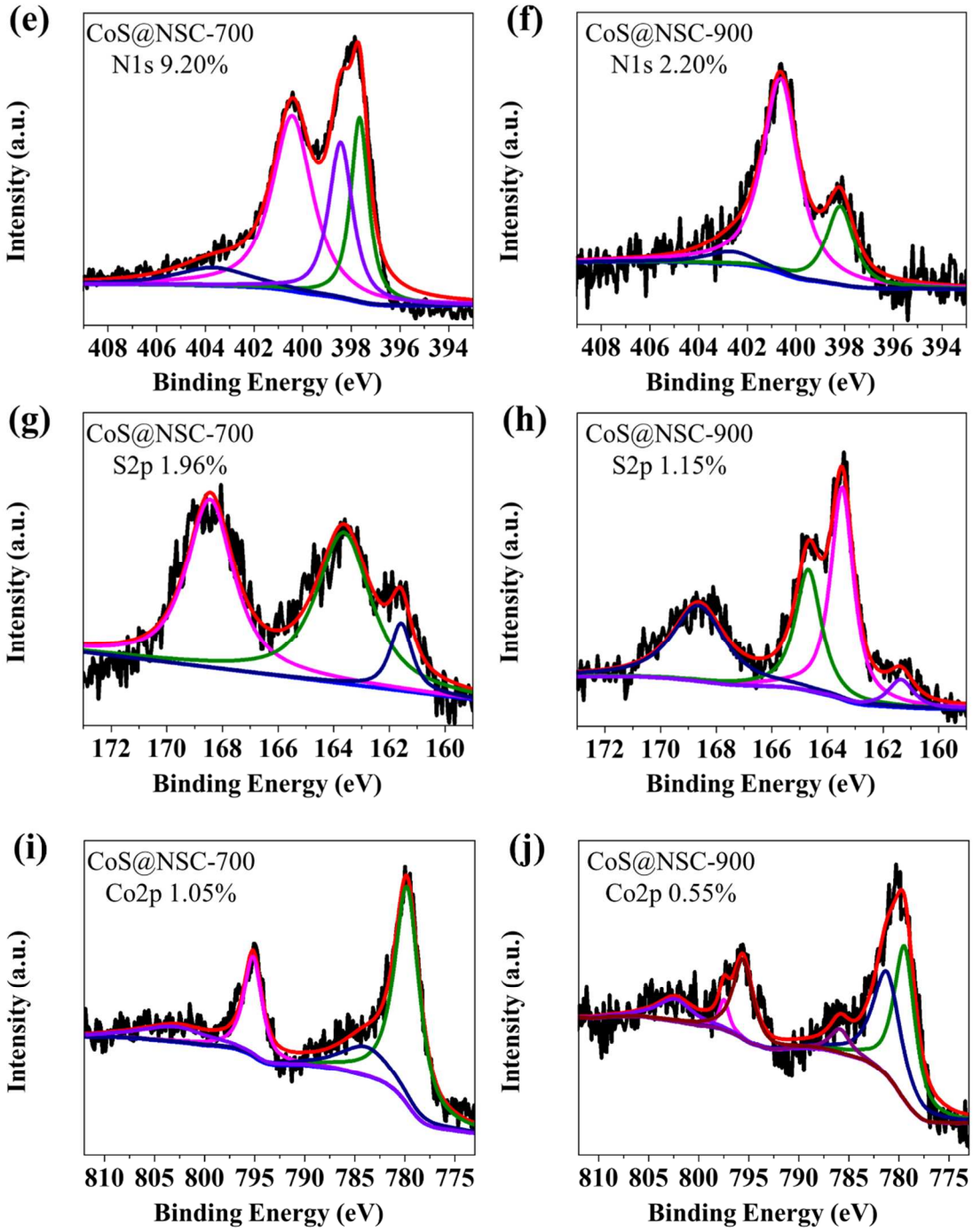

Figure S5. high-resolution spectra of (a, b) C1s, (c, d) O1s, (e, f) N1s, (g, h) S2p, and (i, j) Co2p3 for the as-prepared CoS@NSC-700 and CoS@NSC-900, respectively.

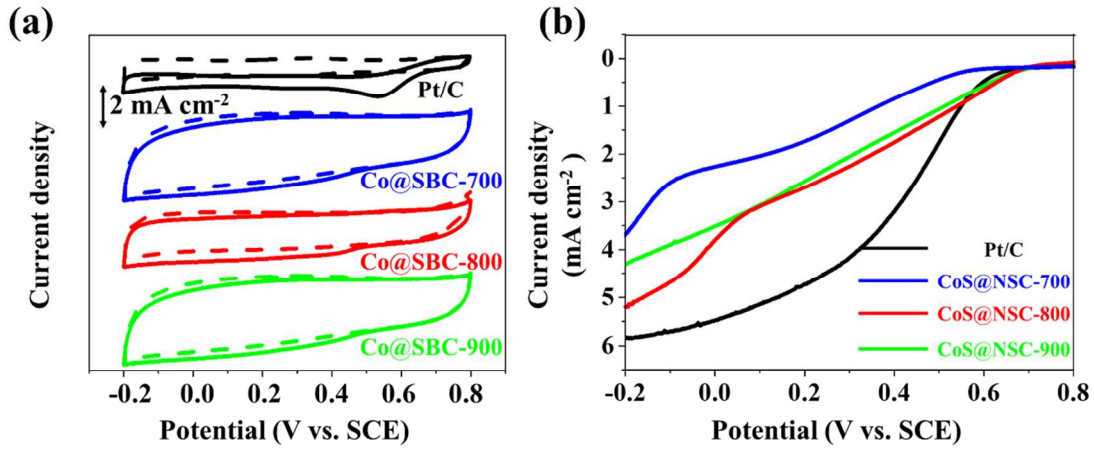

Figure S6. (a) CV curves of CoS@NSC-700, CoS@NSC-800, CoS@NSC-900 and commercial Pt/C in O_2 (solid lines) or N_2 (dash lines) saturated 0.1 M $HClO_4$ solution with a scan rate of 50 mV S^{-1}. (b) LSV curves of of CoS@NSC-700, CoS@NSC-800, CoS@NSC-900 and Pt/C catalysts on RDE in O_2 saturated 0.1 M $HClO_4$ solution with a scan rate of 10 mV S^{-1} and rotation speed of 2000 rpm.

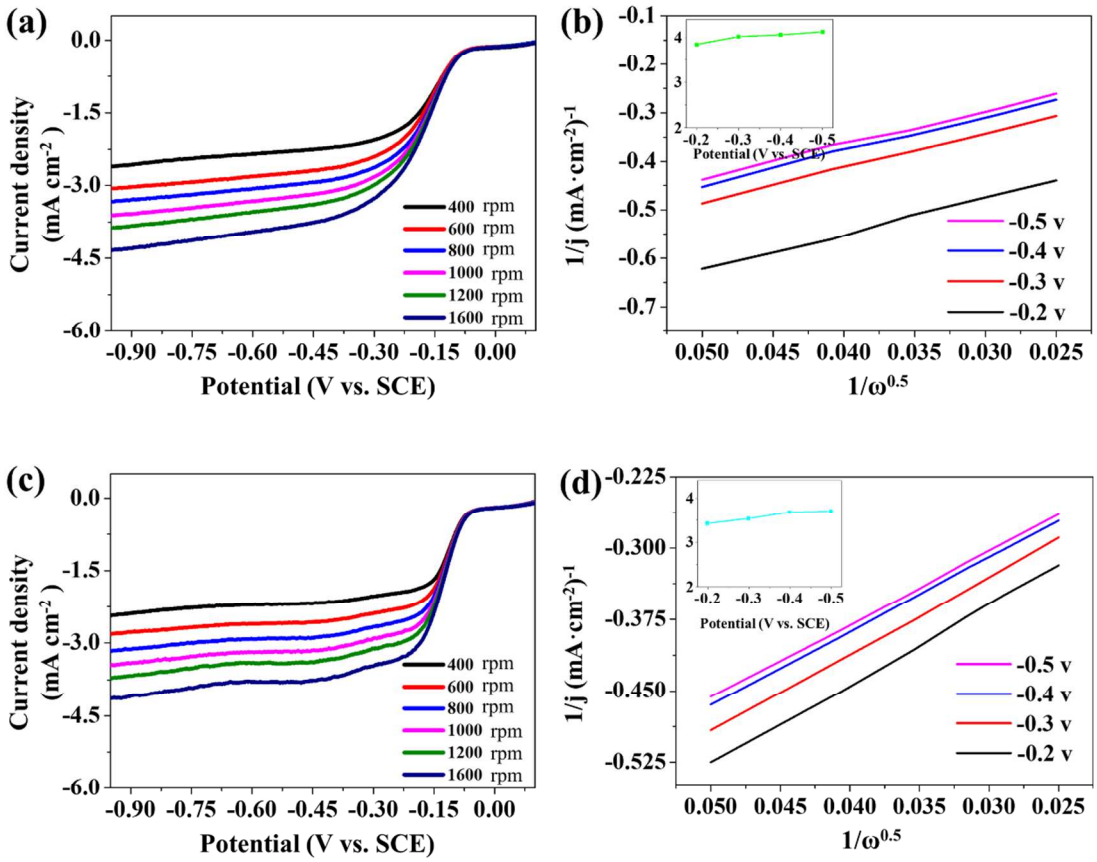

Figure S7. The LSV curves of CoS@NSC-700 (a) and CoS@NSC-900 (c) at rotation speed from 400 to 1600 rpm in the O_2 saturated 0.1M KOH solution at the scan rate of 10 mVs^{-1}. The K-L plots of CoS@NSC-700 (c) and CoS@NSC-900 (d), inset: the electron transfer number at different electrode potentials.

Table S3. ORR electrocatalytic activity comparison between CoS@NSC-800 and other transitional metal catalysts at rotation speed of 1600 rpm in the O_2 saturated 0.1M KOH solution.

Sample	Loading amount mg cm^{-2}	Half-wave potential V	Limit current density mA cm^{-2}	Current density per loading mA/mg
CoS@NSC-800	0.3	-0.134	-5.4	-18
$Co@Co_3O_4@PPD$[34]	0.25	-0.141	-4.23	-16.92
$CoS_2(400)/N,S-GO$[38]	0.25	-0.22	-4.29	-17.16
$NiCo_2O_4–G$[46]	0.4	-0.316	-4.21	-10.525
Fe–N–C[58]	0.2	-0.172	-4.96	-24.8
N-Co9S8/G[62]	0.2	-0.245	-5.7	-28.5
$Co_{0.5}Fe_{0.5}S@N-MC$[63]	0.8	-0.182	-5	-6.25

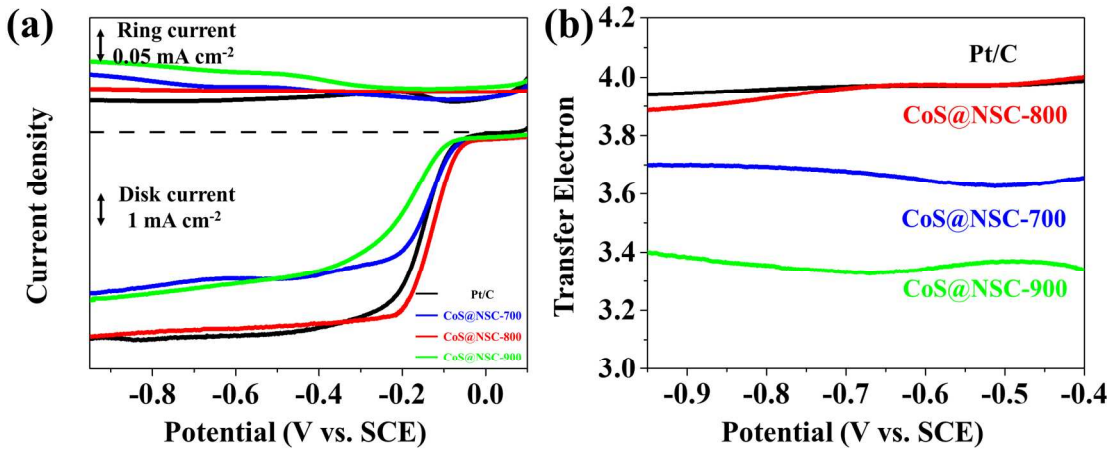

Figure S8. The LSV curves of CoS@NSC-700, CoS@NSC-800, CoS@NSC-900 and Pt/C catalysts on a glassy carbon rotating ring-disk electrode (RRDE) in O_2 saturated 0.1 M KOH solution with a scan rate of 10 mV s^{-1} and rotation speed of 2000 rpm.

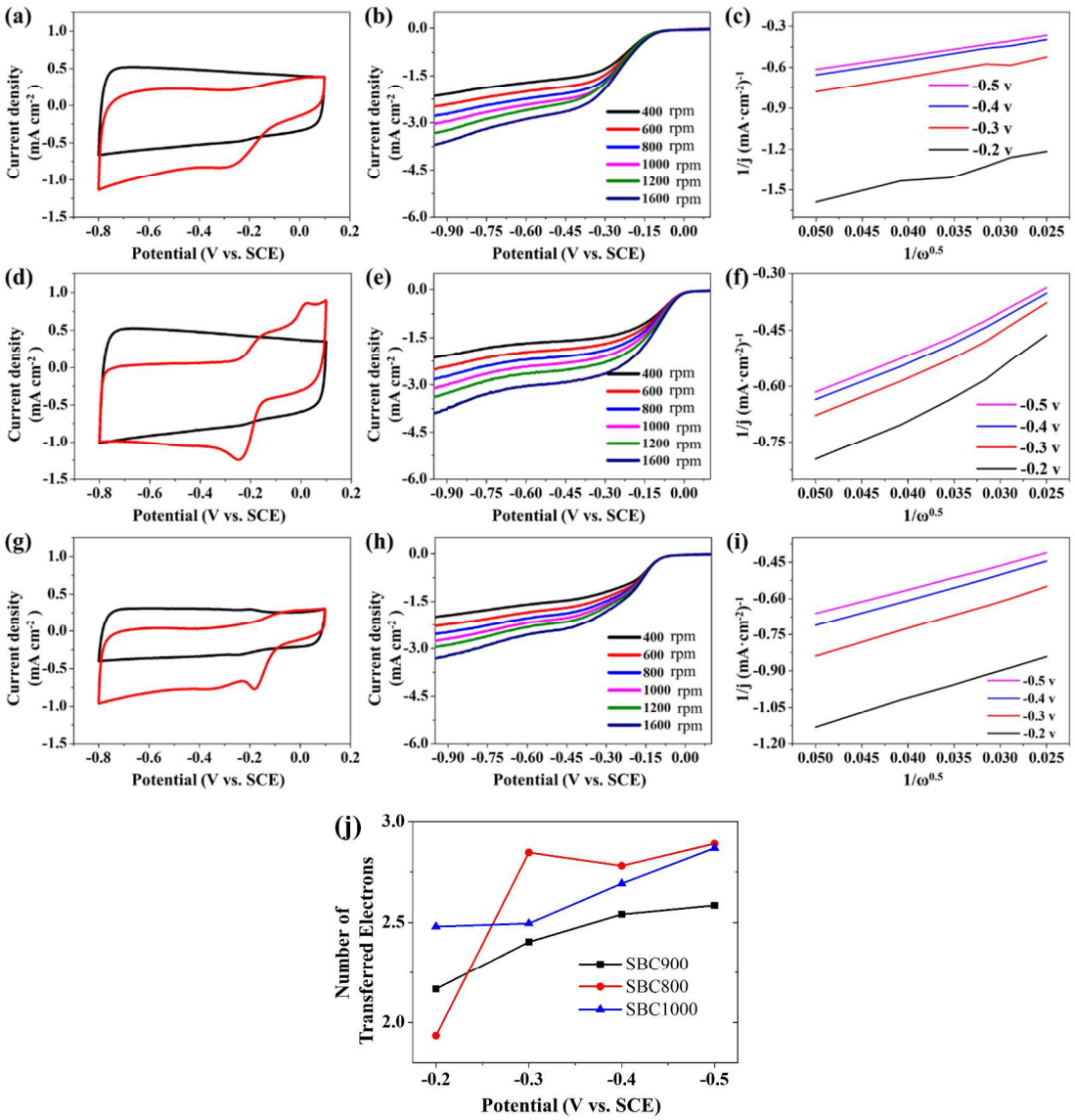

Figure S9. CV and LSV curves and the K-L plots of NSC-700 (a, b, c), NSC-800 (d, e, f) and NSC-900 (g, h, i) in O_2-saturated 0.1 M KOH solution. Electron transfer number of NSC-700, NSC-800 and NSC-900 at different electrode potential (j).

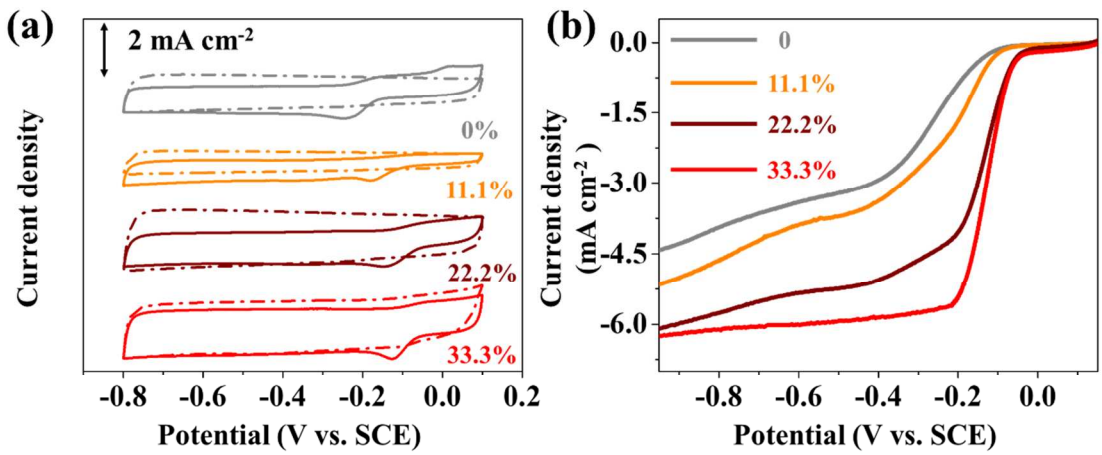

Figure S10. CV and LSV curves of the samples treated by $Co(NO_3)_2$ aqueous solution with various mass fraction of 0%, 11.1%, 22.2% and 33.3% which were carbonized at 800 °C.

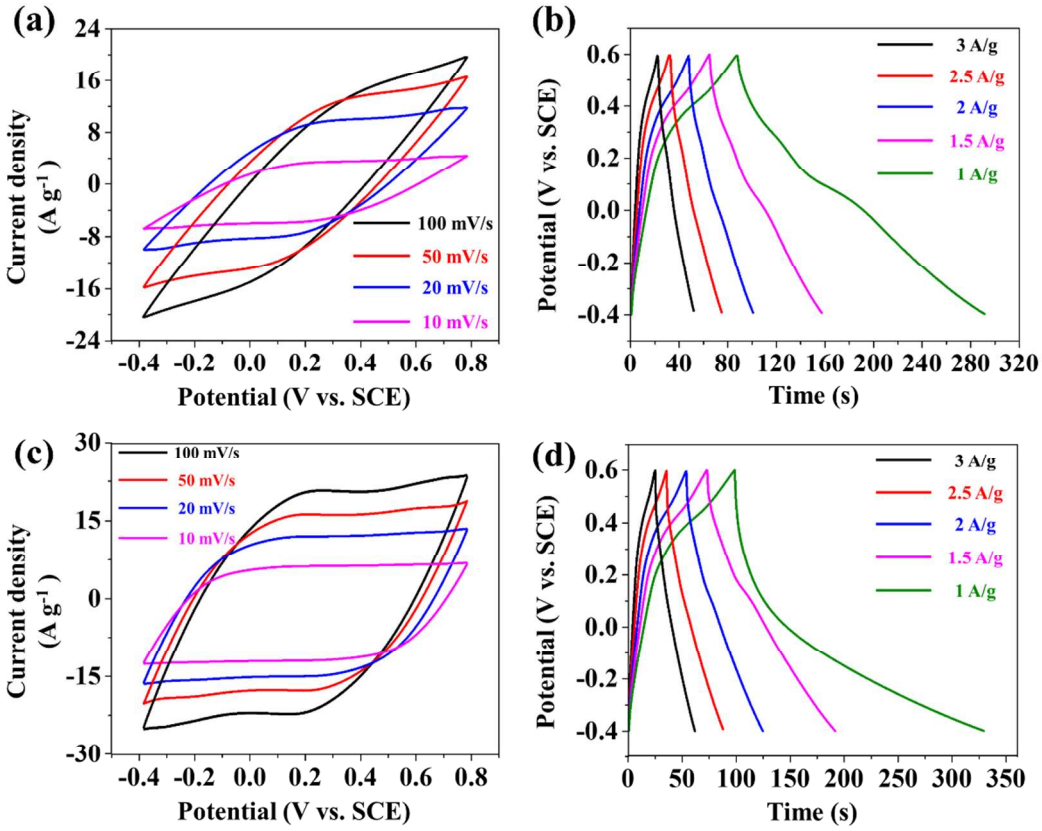

Figure S11. CV curve of CoS@NSC-700 (a) and CoS@NSC-900 (c) at different scan rate from 10 to 100 mV S^{-1}. Galvanostatic charge/discharge curves of CoS@NSC-700 (b) and CoS@NSC-900 (d) with different current density at a potential window of -0.4 V to 0.6 V in 6 M KOH solution.

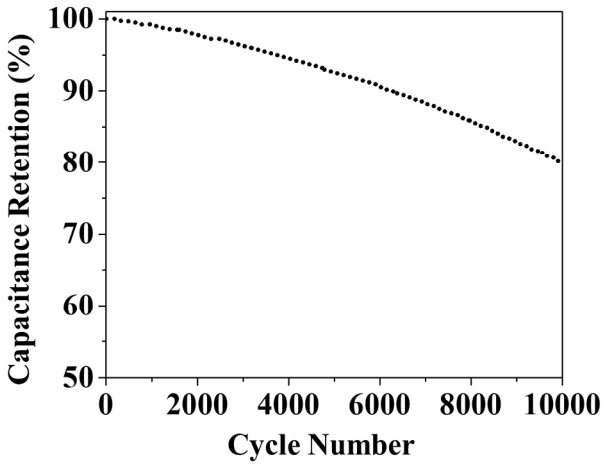

Figure S12. Cyclic stability of CoS@NSC-800 with a current density of 5 A/g in 6 M KOH solution at room temperature.